Facile Electrosynthesis of Fe_3O_4 Nanoparticles Mediated with Sodium Alginate for Paracetamol Degradation

A Masudi [1], N. W. C Jusoh [1,2], P Y Liew [1]

[1] Department of Chemical Process Engineering, Malaysia Japan International Institute ofTechnology, (MJIIT), Universiti Teknologi Malaysia Kuala Lumpur, Jalan Sultan Yahya Petra, 54100 Kuala Lumpur, Malaysia
[2] Center of Hydrogen Energy, Institute of Future Energy, Universiti Teknologi Malaysia Kuala Lumpur, Jalan Sultan Yahya Petra, 54100 Kuala Lumpur, Malaysia

*nurfatehah@utm.my

Abstract. High purity of Fe_3O_4 was prepared by electrochemical method in different concentration of sodium alginate (SA) as natural capping agent. The content of SA influenced the particle size and surface interaction to Fe_3O_4 as confirmed by X-ray diffraction (XRD) and Fourier Transform Infrared (FTIR) spectroscopy. The highest photocatalytic activity was obtained for Fe_3O_4 synthesized with 0.05% SA with initial concentration of 15 mg/L Paracetamol. This result contributed to electrochemical advancement to produce Fe_3O_4 with simple method.

1. Introduction

The occurrence of some organic contaminants in water became one of primary concern with increasing priority to environment sustainability. The contaminants include pharmaceutical, industrial chemical, pesticides and emerging compounds. The pharmaceutical industry increases almost 10% yearly in Malaysia. This continuous elevating demand, generated pharmaceutical discharge to environment. Paracetamol (PCT) is the largest analgesic and antipyretic drug without prescription worldwide which could be utilized as model of pharmaceutical waste. PCT was detected in the range of 0.22-6.8 μg/L in Spain [1], 0.033-0.071 μg/L in South Korean's surface water [2] and 0.01-0.07 μg/L in surface and sewage water in Malaysia [3].

Water quality could be improved by several techniques such as adsorption, biological and membrane. The former method actually only transfer pollutant to other materials and require additional post-treatment [4]. Biological route was ineffective for antibacterial drug [5], while membrane was limited by membrane fouling and high cost [6]. A promising method to degrade pollutants was based on advanced oxidation process (AOPs) which produced many reactive compounds. As part of AOPs, photocatalyst attract many researchers due to its simplicity to degrade pollutant with only assistance of light and a catalyst. However, the commercial catalysts were difficult to separate which increase the operational cost [7]. Fe_3O_4 is one of promising catalyst with easy recovery using external magnet. Zaidi et al [8] verified that the magnetic separation is more affordable than conventional filtration method.

There are many methods to synthesis nanosizes of Fe_3O_4 such as sol-gel [9], hydrothermal [10] and co-precipitation [11]. However, these routes require complex experimental set up and high temperature. Electrochemical method is one alternative to produce metal oxides and composites at low temperature. However, the existing electrochemical route require an ionic liquid such as 1-butyl-3-methyl-imidazolium chloride ([BMIM]Cl) [12]. Thus, its crucial to obtain low cost material to substitute the ionic liquid. The general role of ionic liquid is as a capping agent to produce nanoscale material. Some

studies have been reported that urea and poly ethylene glycol (PEG) [13], seaweed [14] and sodium alginate [15] as promising capping agents. Sodium alginate (SA) not only reported as capping agent in single metal oxide or composite, but also assist adsorption to heavy metals [16]. To the best of our knowledge, a detail study on interaction between capping agent and catalyst still scarce in literatures. The aims of this study is to provide an insight to reagents interaction during the synthesis and photocatalytic activity to degrade PCT.

2. Experimental

2.1. Synthesis Method

The Fe_3O_4 synthesis method was conducted in one compartment and open air at 0 °C contain 1 M TEAP with a series concentration of SA (0, 0.01, 0.05 and 0.1 % w/v). The same size of iron and platinum (2×2 cm^2) as anode and cathode were placed in parallel position. Prior to electrolysis, pH was fixed at 9 in constant current density of 120 mA/cm^2 with continuous stir at 250 rpm. The obtained precipitate was washed with water and ethanol three times, respectively. The black powder was then dried at 60 °C overnight to remove the impurities. The sample was denoted as x% SA. Fe_3O_4, where x indicated the concentration of SA.

2.2. Characterization

The crystallinity and phase purity of the catalysts was measured by X-ray diffraction (XRD) D8 Advance Bruker in the range of 20-90 °. Joint committee on powder diffraction (JCPDS) was used to ensure the phases of the samples. Vibrational spectroscopy of the catalyst was recognized with Fourier transform infrared (FTIR) Shimadzu IRT Tracer-100 at wavelength scan of 400-4000 cm^{-1} using KBr pellet. The, the morphologies of the catalysts were visualized with FESEM JEOL JFC-1600.

2.3. Photodegradation Studies to Paracetamol

The photoactivity of the catalyst was evaluated to degrade paracetamol (PCT). The catalyst was placed in a dark condition for 1 h to obtain equilibrium of adsorption-desorption between catalyst and solution. Then, this suspension was exposed by simulated light for 2 h. The initial concentration of PCT was fixed at 15 mg/L. The concentration of PCT during reaction was then monitored by UV-vis Shimadzu at 244 nm. Each experiment was conducted three times to ensure the accuracy of the data. This procedure was replicated for all the studied parameter to elucidate the effect of pH, SA concentration and catalyst dosage.

3. Result and Discussion

3.1. Crystallinity and Phase Purity

Figure 1 shows the XRD pattern of Fe_3O_4 with a series concentration of SA. The peaks appeared at 30.2, 35.6, 43.2, 54.92, 57.4 and 62.9 ° assigned to (220), (311), (400), (422), (511) and (440) planes. These peaks match with JCPDS. card 19-062 attributed to Fe_3O_4 with inverse spinel structure [17]. As presented in Table 1, the crystallite size of Fe_3O_4 using Scherrer equation are in nanoscale. The use of low temperature during drying may cause larger crystallite size of Fe_3O_4 with SA than without SA (Fe_3O_4), due to the remaining of SA on Fe_3O_4 surface. The product was not calcined as the Fe_3O_4 may transform to other iron oxide phases. As displayed in Figure 1 (a), Fe_3O_4 without SA has very low crystallinity. Then, the crystallinity increased significantly after addition of low content of SA (0.01%). By increasing the content of SA to 0.05%, the crystal size of Fe_3O_4 decreased indicating that SA may cover entirely the Fe_3O_4 nuclei. However, at higher concentration of SA (0.1%), the particle size increased again as a result of attraction between excessive alginate chains to sodium ions which further agglomerated and became larger size [18].

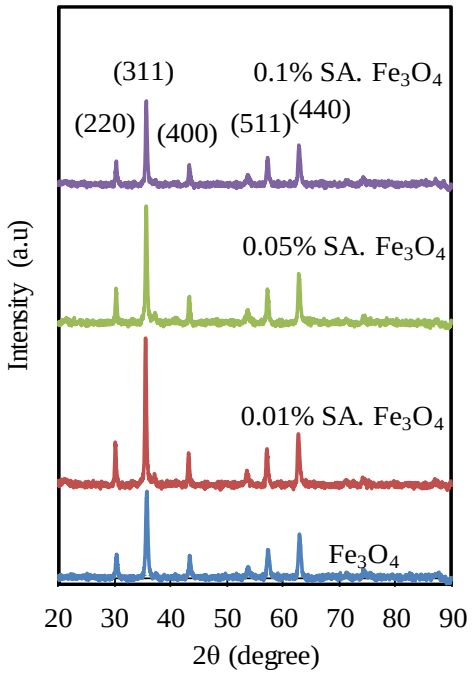

Figure 1. XRD pattern of Fe_3O_4 with various SA concentration

Table 1. Crystallite particle size of Fe_3O_4 in various SA concentration

Catalyst type	Concentration of sodium alginate (%w/v)	Size (nm)
Fe_3O_4	0	28.41
0.01% SA.Fe_3O_4	0.01	37.82
0.05% SA.Fe_3O_4	0.05	30.96
0.1% SA.Fe_3O_4	0.1	34.09

3.2. Vibrational Spectroscopy

Figure 2 displays FTIR spectra of the catalyst to obtain the chemical interaction between SA and Fe_3O_4. The spectra of SA comprised of 1093 and 1030 cm^{-1} assigned to C-O-C of saccharide structure. The band at 1417 and 1620 cm^{-1} are asymmetric and symmetric stretching vibration of carboxyl groups. Then, peaks at 2930 and 3340 cm^{-1} associated to stretching vibration of O-H and C-H [19]. The characteristic of Fe-O bond vibration appeared at 624 cm^{-1} in all catalysts. Then, new peaks were observed in 798 and 1120 cm^{-1} with low intensity in 0.01% catalyst which may be assigned to interaction between SA and Fe-O. These peaks became more intense at 0.05% catalyst which may be indicated as more SA bonding to Fe-O. The intensities of these new peaks were then decreased in 0.1% catalyst. This may be a sign that bonding between Fe_3O_4 and SA not as much as 0.05% catalyst [20].

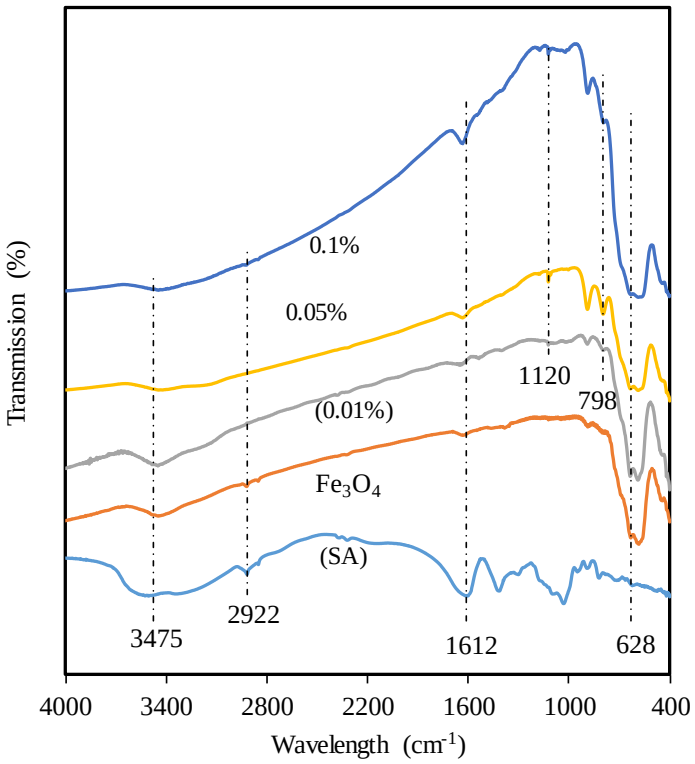

Figure 2. FTIR spectra of Fe_3O_4 with various SA concentration

3.3. Morphological Studies

The morphologies of 0.05% SA. Fe_3O_4 and Fe_3O_4 were investigated with field emission scanning electron microscopy (FESEM). The observation confirmed that the catalysts are spherical in shape. This result is similar with Esmat et al. From these figures, it was observed that Fe_3O_4 in presence of SA has lower agglomeration than Fe_3O_4.

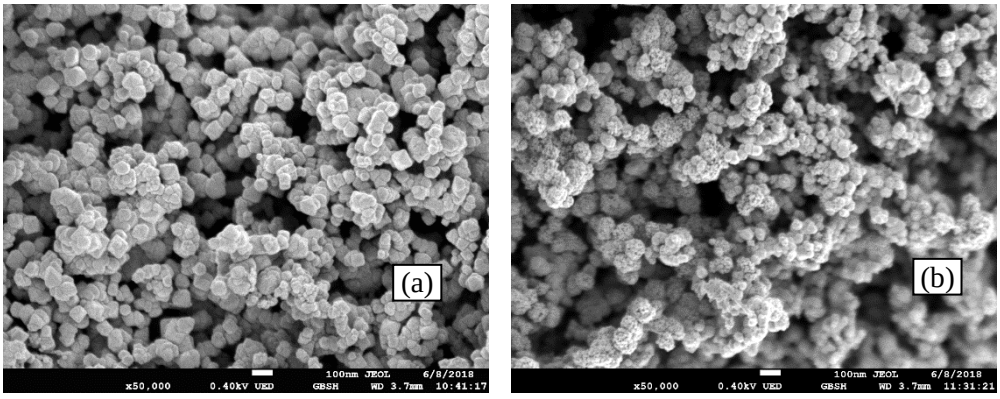

Figure 3. FESEM images of (a) 0.05% SA. Fe_3O_4 and (b) Fe_3O_4

3.4. Photocatalytic Degradation

The photocatalytic activities were examined under several parameters such as effect of pH, SA concentration and catalyst dosage. These parameters were useful to obtain optimum condition for PCT degradation.

3.4.1. Effect of pH

pH of aqueous solution influenced the pollutant interaction to the catalyst surface. A typical semiconductor catalyst behaved as amphoteric depend on the environmental pH. In this study, the effect of pH was examined in the range of 5-9 as presented in Figure 3. The highest degradation rate was obtained at pH 9 where the Fe_3O_4 and PCT were negative and positively charged, respectively [21]. Meanwhile, both of Fe_3O_4 and PCT were in the same charge in other pH which further repel each other, then minimize the PCT degradation.

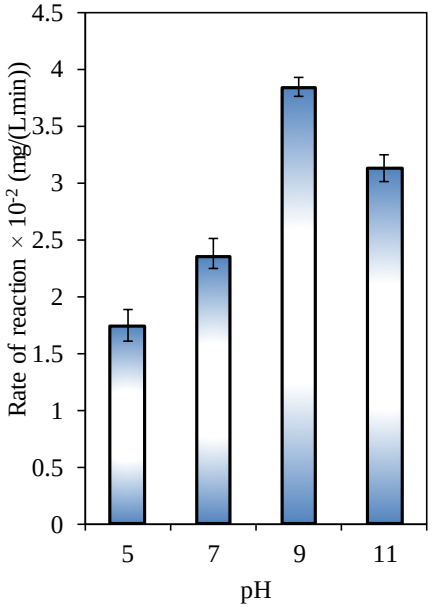

Figure 4. Effect of pH in PCT degradation

3.4.2. Effect of SA concentration

SA content played a crucial role for Fe_3O_4 formation. The different concentration of SA produced different size and interaction between catalyst and SA which further affected the photocatalytic activity as presented in Figure 5. The degradation rate of Fe_3O_4 without SA was higher than in presence of 0.01% SA may be attributed to its smaller particle size. Then, the degradation rate increased drastically as a result of small particle size when using 0.05% SA. Last, the degradation rate decreased when added more SA (0.1% w/v) due to their larger particle size. This assumption was strengthened by Aziz et al [22], where small particle size will result higher photodegradation performances. The presence of SA in Fe_3O_4 surface was crucial to enhance the adsorption of malachite green such as reported by [18], azo dye in gold-alginate [23] and selective removal of heavy metals (Pb^{2+}, Cu^{2+}, Cd^{2+}) [24]. Additionally, the formation of new bonds at 1120 cm^{-1} and 798 cm^{-1} indicated that SA was might be covalently bonded to Fe_3O_4 surface. These new bonds were considered as key role for enhanced paracetamol degradation. This result was aligned with research by Soares et al [25] where carrageenan was successfully grafted to siliceous Fe_3O_4 and produce robust, stable and reusable for methylene blue (MB) adsorption. Carrageenan is similar with SA in term of chemical structure and also family of polysaccharides. In this study, SA was attached to carboxyl and ether functional groups as hypothesized with FTIR. At low content of SA (0.01% w/v), new bonds were started to appear with small intensity, then become more intense using 0.05% of SA. However, at higher concentration (0.1%), the intensity reduced and followed

with sharper intensity in carboxyl group. This phenomena indicated that new bond formation with SA as active site for PCT degradation which may decrease at high concentration of SA due to accumulation of alginate chain attach to sodium ions as reported in the literature [18].

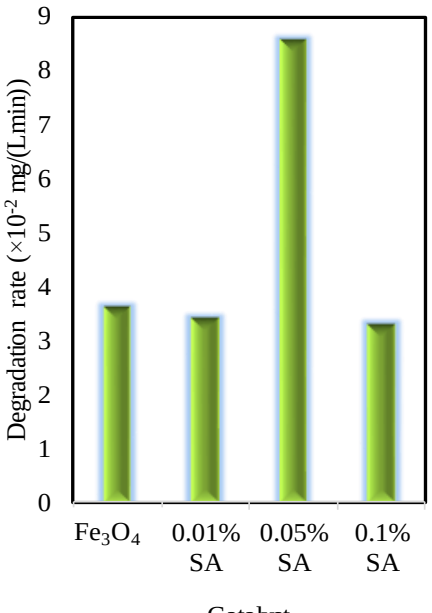

Figure 5. Effect of SA concentration in PCT degradation

3.4.3. Effect of catalyst dosage

The effect of catalyst dosage is presented in Figure 6. Catalyst dosage play vital role in pollutant degradation, especially in industrial scale. The presence of more Fe_3O_4 enhanced the photon absorption over catalyst surface and reach optimum degradation at 0.45 g/L. The degradation rate decreased at higher catalyst dosage due to excessive black opaque of Fe_3O_4 which hindered light penetration to Fe_3O_4 surface [26].

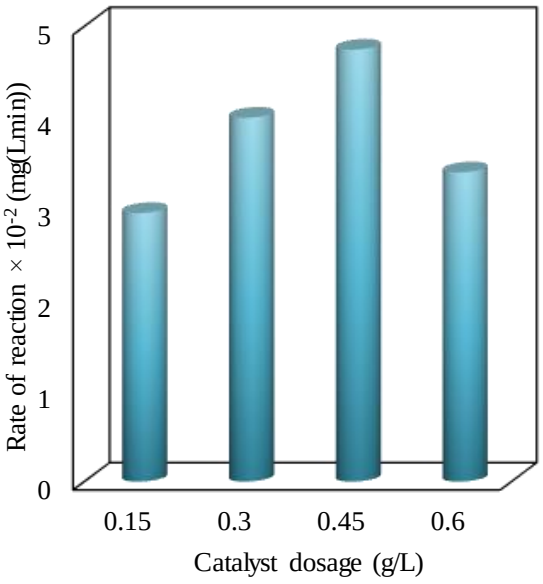

Figure 6. Effect of catalyst dosage in PCT degradation

4. Conclusion

A series of Fe_3O_4 was successfully prepared with electrochemical method with various concentration of SA. SA could control the particle size of Fe_3O_4 of which the interaction affected by the content of SA. The optimum degradation rate towards Paracetamol was obtained for 0.05% SA. Fe_3O_4 with 0.45 g/L of the catalyst at pH 9.

Acknowledgment

This research was supported by Ministry of Education (MOE) through Fundamental Research Grant Scheme (FRGS/1/2018/STG07/UTM/02/11). and MJIIT Incentive Scheme (Ahmad Masudi) from MJIIT UTM.

References

[1] Gómez M J, Martínez Bueno M J, Lacorte S, Fernández-Alba A R and Agüera A 2007 Pilot survey monitoring pharmaceuticals and related compounds in a sewage treatment plant located on the Mediterranean coast *Chemosphere* **66** 993-1002

[2] Kim S D, Cho J, Kim I S, Vanderford B J and Snyder S A 2007 Occurrence and removal of pharmaceuticals and endocrine disruptors in South Korean surface, drinking, and waste waters *Water Research* **41** 1013-21

[3] Al-Odaini N A, Zakaria M P, Yaziz M I and Surif S 2010 Multi-residue analytical method for human pharmaceuticals and synthetic hormones in river water and sewage effluents by solid-phase extraction and liquid chromatography–tandem mass spectrometry *Journal of Chromatography A* **1217** 6791-806

[4] Zou W, Gao B, Ok Y S and Dong L 2019 Integrated adsorption and photocatalytic degradation of volatile organic compounds (VOCs) using carbon-based nanocomposites: A critical review. Elsevier Ltd) pp 845-59

[5] Baêta B E L, Lima D R S, Silva S Q and Aquino S F 2015 Evaluation of soluble microbial products and aromatic amines accumulation during a combined anaerobic/aerobic treatment of a model azo dye *Chemical Engineering Journal* **259** 936-44

[6] Dharupaneedi S P, Nataraj S K, Nadagouda M, Reddy K R, Shukla S S and Aminabhavi T M 2019 Membrane-based separation of potential emerging pollutants. Elsevier) pp 850-66

[7] Sidik D A B, Hairom N H H, Zainuri N Z, Desa A L, Misdan N, Yusof N, Ong C B, Mohammad A W and Aripen N S M 2018 Photocatalytic degradation of industrial dye wastewater using zinc oxide-polyvinylpyrrolidone nanoparticles *Malaysian Journal of Analytical Sciences* **22** 693-701

[8] Zaidi N S, Sohaili J, Muda K and Sillanpää M 2014 Magnetic field application and its potential in water and wastewater treatment systems. pp 206-40

[9] Omri K, Sajieddine M, Bououdina M, El Mir L, Zhang B, Lemine O M and Alyamani A 2012 Sol–gel synthesis of 8nm magnetite (Fe3O4) nanoparticles and their magnetic properties *Superlattices and Microstructures* **52** 793-9

[10] Zhang H and Zhu G 2012 One-step hydrothermal synthesis of magnetic Fe 3 O 4 nanoparticles immobilized on polyamide fabric *Applied Surface Science* **258** 4952-9

[11] Aphesteguy J C, Kurlyandskaya G V, De Celis J P, Safronov A P and Schegoleva N N 2015 Magnetite nanoparticles prepared by co-precipitation method in different conditions *Materials Chemistry and Physics* **161** 243-9

[12] Li Y, Qiang Q, Zheng X and Wang Z 2015 Controllable electrochemical synthesis of Ag nanoparticles in ionic liquid microemulsions *Electrochem. Commun.* **58** 41-5

[13] Ibrahim N A, Nada A A, Hassabo A G, Eid B M, Noor El-Deen A M and Abou-Zeid N Y 2017 Effect of different capping agents on physicochemical and antimicrobial properties of ZnO nanoparticles *Chem. Pap.* **71** 1365-75

[14] Kannan R R R, Stirk W A and Van Staden J 2013 Synthesis of silver nanoparticles using the seaweed Codium capitatum P.C. Silva (Chlorophyceae) *South African Journal of Botany* **86** 1-4

[15] Chunfa D, Xianglin Z, Hao C and Chuanliang C 2016 Sodium Alginate Mediated Route for the Synthesis of Monodisperse Silver Nanoparticles Using Glucose as Reducing Agents *Rare Metal Materials and Engineering* **45** 261-6
[16] Esmat M, Farghali A A, Khedr M H and El-Sherbiny I M 2017 Alginate-based nanocomposites for efficient removal of heavy metal ions *International Journal of Biological Macromolecules* **102** 272-83
[17] Areerob Y, Cho J Y, Jang W K and Oh W-C 2018 Enhanced sonocatalytic degradation of organic dyes from aqueous solutions by novel synthesis of mesoporous Fe3O4-graphene/ZnO@SiO2 nanocomposites *Ultrasonics Sonochemistry* **41** 267-78
[18] Daemi H and Barikani M 2012 Synthesis and characterization of calcium alginate nanoparticles, sodium homopolymannuronate salt and its calcium nanoparticles *Scientia Iranica* **19** 2023-8
[19] Qiao X, Niu L, Zhang H, Wen X, Cao Y and Bai G 2017 Controllable fabrication of a novel porous Ni-alginate hybrid material for hydrogenation *Applied Catalysis B: Environmental* **218** 721-30
[20] Hussein-Al-Ali S H, El Zowalaty M E, Hussein M Z, Ismail M, Dorniani D and Webster T J 2014 Novel kojic acid-polymer-based magnetic nanocomposites for medical applications *International journal of nanomedicine* **9** 351-62
[21] Tan C, Gao N, Deng Y, Deng J, Zhou S, Li J and Xin X 2014 Radical induced degradation of acetaminophen with Fe3O4 magnetic nanoparticles as heterogeneous activator of peroxymonosulfate *Journal of Hazardous Materials* **276** 452-60
[22] Aziz F F A, Jalil A A, Triwahyono S and Mohamed M 2018 Controllable structure of fibrous SiO2–ZSM-5 support decorated with TiO2 catalysts for enhanced photodegradation of paracetamol *Applied Surface Science* **455** 84-95
[23] Li Y, Li G, Li W, Yang F and Liu H 2015 Greenly Synthesized Gold–Alginate Nanocomposites Catalyst for Reducing Decoloration of Azo-Dyes *Nano* **10** 1550108
[24] Wang F, Lu X and Li X-y 2016 Selective removals of heavy metals (Pb2+, Cu2+, and Cd2+) from wastewater by gelation with alginate for effective metal recovery *Journal of Hazardous Materials* **308** 75-83
[25] Soares S F, Simões T R, Trindade T and Daniel-da-Silva A L 2017 Highly Efficient Removal of Dye from Water Using Magnetic Carrageenan/Silica Hybrid Nano-adsorbents *Water, Air, & Soil Pollution* **228** 87
[26] Hassani A, Karaca C, Karaca S, Khataee A, Açışlı Ö and Yılmaz B 2018 Enhanced removal of basic violet 10 by heterogeneous sono-Fenton process using magnetite nanoparticles *Ultrasonics Sonochemistry* **42** 390-402